

Synthesis of $\text{Ca}_{2-x}\text{Sr}_x\text{CuO}_2\text{F}_2$ ($0 \leq x \leq 2$) with the T'-structure through fluorination of $\text{Ca}_{2-x}\text{Sr}_x\text{CuO}_3$ with poly(vinylidene fluoride)/poly(tetrafluoroethylene)

R. Heap¹ and P.R. Slater^{2*}

¹Chemical Sciences, University of Surrey, Guildford, Surrey, GU2 7XH, UK

²School of Chemistry, University of Birmingham, Birmingham B15 2TT. UK

*Correspondence to: Prof. P.R. Slater

School of Chemistry, University of Birmingham, Birmingham B15 2TT. UK

Tel. +44 (0)121 4148906

Fax +44 (0)121 4144403

p.r.slater@bham.ac.uk

This paper is copyright Prof. P.R. Slater

Abstract

In this paper, the synthesis of the series, $\text{Ca}_{2-x}\text{Sr}_x\text{CuO}_2\text{F}_2$ ($0 \leq x \leq 2$), is reported by the fluorination of $\text{Ca}_{2-x}\text{Sr}_x\text{CuO}_3$ starting materials with poly(vinylidene fluoride)/poly(tetrafluoroethene). The structural refinements showed that all samples adopt the T'-structure, in contrast to the previous observation of the T-structure for $\text{Sr}_2\text{CuO}_2\text{F}_{2+\delta}$, when the phase is synthesised using F_2 gas. The difference can be related to the lack of interstitial fluoride ions ($\delta = 0$) in the samples synthesised via fluorination with the polymers, and hence highlights that the T-structure is only formed if there is partial oxidation of Cu through incorporation of interstitial fluoride ions ($\delta > 0$), as is the case when F_2 gas is employed.

1. Introduction

Since the discovery of high-temperature superconductivity in $\text{Sr}_2\text{CuO}_2\text{F}_{2+\delta}$ [1], there has been considerable interest in related alkaline earth copper oxide fluorides [2-29]. The synthesis of these materials has, however, proved particularly troublesome as they are not stable at high temperatures. Thus heating to elevated temperatures results in decomposition to give alkaline earth fluoride impurities. Therefore, the synthesis is typically carried out in two stages: the production of an oxide precursor, followed by low temperature fluorination of this oxide. Despite the large interest in these systems, comparatively little has been done on investigating the structural changes for the series $\text{Sr}_{2-x}\text{Ca}_x\text{CuO}_2\text{F}_{2+\delta}$, apart from the two end-members ($x=0, 2$). For these two systems, it has been shown that $\text{Ca}_2\text{CuO}_2\text{F}_2$ is non-superconducting and displays the T' -structure (Nd_2CuO_4 - type) as shown in Figure 1, whereas $\text{Sr}_2\text{CuO}_2\text{F}_{2+\delta}$, as mentioned above, is superconducting at 46K and displays the T-structure (La_2CuO_4 - type) as shown in Figure 2. In an attempt to determine what influences this crossover in structure type, and at what Ca:Sr ratio it occurs, a synthesis and structural investigation of the $\text{Ca}_{2-x}\text{Sr}_x\text{CuO}_2\text{F}_{2+\delta}$ ($0 \leq x \leq 2$) series was undertaken. This involved the initial synthesis of the precursor oxides, $\text{Ca}_{2-x}\text{Sr}_x\text{CuO}_3$, followed by fluorination using polymer-based fluorinating agents. The materials have been structurally characterised by the Rietveld refinement of X-ray and neutron powder diffraction data. The polymer-based fluorination method has been shown to be an excellent route to the synthesis of mixed metal oxide fluoride systems, tending to produce higher quality samples with reduced metal fluoride impurities compared to other low temperature fluorination methods [30-35].

2 Experimental

High purity CaCO_3 , SrCO_3 and CuO were intimately ground in the correct ratio to produce $\text{Ca}_{2-x}\text{Sr}_x\text{CuO}_3$ where $x = 0.0, 0.25, 0.5, 0.75, 1.0, 1.25, 1.5, 1.75,$ and 2.0 . These mixtures were heated at temperatures between 950°C and 1050°C for 16 hours before being reground and reheated under the same conditions. The samples were characterised using XRD (Panalytical X'Pert Pro diffractometer with $\text{Cu K}\alpha_1$ radiation), which showed the successful synthesis of all phases. As expected from cation size considerations, there is a shift in the peaks to lower angles with increasing Sr content (Figure 3), indicating an increase in unit cell size.

With the successful synthesis of the oxide precursors, attempts were then made to fluorinate these parent materials using poly(vinylidene fluoride) (PVDF). The $\text{Ca}_{2-x}\text{Sr}_x\text{CuO}_3$ samples were intimately ground with PVDF, using a pestle and mortar, in the correct ratio to produce $\text{Ca}_{2-x}\text{Sr}_x\text{CuO}_2\text{F}_2$ (i.e. 1:1 ratio of $\text{Ca}_{2-x}\text{Sr}_x\text{CuO}_3 : \text{CH}_2\text{CF}_2$ monomer unit). Note that as PVDF is a non-oxidative fluorinating agent, it was expected that that the fully stoichiometric $\text{Ca}_{2-x}\text{Sr}_x\text{CuO}_2\text{F}_2$ system would be produced with no interstitial F. The fluorination was performed in a furnace placed within a fume cupboard, to ensure safe removal of the polymer decomposition products.

Initial fluorination attempts employed a reaction temperature of 325°C , but showed generally poor quality samples, with the strong presence of Sr/ CaF_2 impurities, the higher the strontium content, the higher were these impurity levels. Therefore the synthesis was repeated, examining a range of fluorinating conditions in order to optimise the synthesis. It was eventually found that most of the parent compounds could be successfully fluorinated by initially using a lower temperature, 250°C for 24 hours,

followed by a gradual increase in temperature up to 360°C over a prolonged period of time, i.e. increments of ~25°C every 24 hours. Unfortunately, the more strontium the samples contained, the more difficulty there was in fluorination using PVDF, such that the successful synthesis with this fluorinating agent was only achieved for $x \leq 1.25$. One possible explanation for the difficulty in synthesising $\text{Ca}_{2-x}\text{Sr}_x\text{CuO}_2\text{F}_2$ with high Sr contents could be the production of H_2O on decomposition of PVDF, resulting in decomposition of the samples. In an attempt to overcome this problem, another fluorine containing polymer, poly-(tetrafluoroethene) (PTFE) was examined for use as a fluorinating agent, since this does not contain hydrogen, and so would not be expected to result in any H_2O by-product. The three phases of $\text{Ca}_{2-x}\text{Sr}_x\text{CuO}_3$, for which fluorination with PVDF had proved unsuccessful ($x = 1.5, 1.75, 2.0$), were therefore ground with powdered PTFE (in the ratio $\text{Ca}_{2-x}\text{Sr}_x\text{CuO}_3 : \text{C}_2\text{F}_4$ monomer unit of 2:1) and heated slowly, with intermittent regrinding and XRD analysis. After initial experimentation with PTFE, it was discovered that, because of the differences in thermal stability between PVDF and PTFE, a higher reaction temperature was required for PTFE. Optimisation of this method resulted in the heat treatments beginning at 325°C, with 25°C increments per 24 hours, up to a maximum temperature of 420°C. This fluorination method allowed the successful fluorination of the three remaining samples although, in the case of $\text{Sr}_2\text{CuO}_2\text{F}_2$ in particular, there were still large SrF_2 impurities. The XRD patterns recorded for all phases in the series $\text{Ca}_{2-x}\text{Sr}_x\text{CuO}_2\text{F}_2$ are shown in Figure 4.

Neutron diffraction data were collected on diffractometer POLARIS, ISIS, Rutherford Appleton Laboratory for 6 samples of $\text{Ca}_{2-x}\text{Sr}_x\text{CuO}_2\text{F}_2$ in the range $0.0 \leq x \leq 1.25$. For the

samples with higher Sr contents ($1.5 \leq x \leq 2.0$), X-ray diffraction data were used for structural analysis. Rietveld refinement was performed for each of the phases in this range using the GSAS suite of programs [36].

3. Results and discussion

The successful synthesis of the series, $\text{Ca}_{2-x}\text{Sr}_x\text{CuO}_2\text{F}_2$ was demonstrated by fluorination of $\text{Ca}_{2-x}\text{Sr}_x\text{CuO}_3$ with PVDF/PTFE. The final refined structural parameters for each phase are given in Table 1 ($0.0 \leq x \leq 1.25$) and Table 2 ($1.5 \leq x \leq 2.0$). An example of the neutron diffraction profiles for one of these phases ($x = 0$) is given in Figure 5. From Figures 4 and 5, it is clear that there are small impurities present in these samples. In particular, for all samples $(\text{Ca}/\text{Sr})\text{F}_2$ impurity were observed, as is common in the synthesis of these phases due to their general metastability [1-4]. The refined structural parameters (Tables 1 and 2) show a number of interesting results. In particular, the expected crossover in structure type from T' to T does not occur. Instead, however, it appears that the materials all conform to the T'-structure. Moreover, there was no evidence for any extra interstitial anions in any sample, indicating a stoichiometric $\text{Ca}_{2-x}\text{Sr}_x\text{CuO}_2\text{F}_2$ composition across the whole range, as expected.

Figures 6(a) and (b) show the variation in unit cell parameters as a function of Sr content. From these data, it is evident that as calcium is replaced by strontium, the unit cell expands as expected, obeying Vegard's law. Lines of best fit drawn through the two data series give R^2 values of 0.9998 and 0.9999 for a and c respectively. The excellent fit

of these data to a straight line is fully consistent with there being no change in structure type across the whole range. The consistency in structure type throughout the range is also reflected in the variation of bond lengths (Figure 7).

The observation of the formation of the T'-structure, on fluorination of $\text{Ca}_{2-x}\text{Sr}_x\text{CuO}_3$ to give $\text{Ca}_{2-x}\text{Sr}_x\text{CuO}_2\text{F}_2$, for the complete range ($0.0 \leq x \leq 2.0$) of samples is very interesting. The structure of the precursor oxide $\text{Ca}_{2-x}\text{Sr}_x\text{CuO}_3$ is related to the K_2NiF_4 structure (figure 8), with rows of equatorial oxygen vacancies running through the structure. As a result of this oxygen deficiency, the system has one-dimensional CuO_4 chains, instead of 2 dimensional layers of CuO_6 octahedra. As can be seen from the results presented here, fluorination of this system has a profound structural effect. The $\text{Ca}_{2-x}\text{Sr}_x\text{CuO}_3$ samples are orthorhombic with cell dimensions $b < a \ll c$. Upon fluorination, the a parameter undergoes a very small expansion, with the smaller b parameter undergoing a larger expansion, as the 1 dimensional CuO_4 chains rearrange to form 2 dimensional CuO_2 layers. Even more interesting though, is the change in the c-parameter across the range (Figure 9). At the Ca-rich end of this series, the c-axis undergoes a contraction upon fluorination. This is to be expected as the CuO_4 chains are transformed into CuO_2 layers. However, the extent of this c-parameter reduction decreases across the range, such that for high Sr levels, a small expansion is observed on fluorination. In contrast, however, to previous work on the fluorination of Sr_2CuO_3 with F_2 , to give $\text{Sr}_2\text{CuO}_2\text{F}_{2+\delta}$ possessing the T-structure [1], the c-axis expansion is much smaller (0.52% versus 5.91%). This is consistent with the formation of $\text{Sr}_2\text{CuO}_2\text{F}_2$ without interstitial F in the present work and the observation of the T'-structure rather than the T-structure, and would suggest that the presence of interstitial F ($\delta > 0$) is what

stabilises the T structure. Further support for this conclusion comes from previous work on the reduction of $\text{Sr}_2\text{CuO}_2\text{F}_{2+\delta}$, with the T-structure, by Kissick *et al.* [20], which showed a transformation to the T'-structure, as interstitial F was lost to give stoichiometric $\text{Sr}_2\text{CuO}_2\text{F}_2$. The cell parameters calculated for $\text{Sr}_2\text{CuO}_2\text{F}_2$ in the present study are very similar to those reported by Kissick *et al.* for their sample after post-synthesis reduction of $\text{Sr}_2\text{CuO}_2\text{F}_{2+\delta}$.

It is also interesting to note that previously, computer modelling studies of $\text{Sr}_2\text{CuO}_2\text{F}_{2+\delta}$ for $\delta=0$ had predicted that the T-structure was more stable than the T'-structure [10,12], whereas the results here suggest the opposite is the case. The discrepancy can be related to the fact that the computer modelling studies determine the theoretical thermodynamically most stable structure, whereas it is known that these systems are metastable, decomposing at higher temperatures with the formation of Sr/CaF₂. The work therefore highlights the dangers of employing modelling studies on inorganic solids synthesised at low temperatures, where kinetics rather than thermodynamics may dictate which structure is formed. In particular, the observation here of the direct formation of the T'-structure may suggest a different fluorination pathway in this non-oxidative fluorination with PVDF/PTFE, compared to fluorination with F₂ gas. In the latter case, it has been proposed that F inserts between the CuO₄ square-planes (figure 8) in the equatorial position between the Cu atoms, producing layers of CuO₄F₂ octahedra and the T-structure. The apical O atoms would then migrate to the equatorial sites and be replaced by F atoms. The new proposed mechanism for the fluorination with these polymer reagents involves F inserting into the interstitial fluorite-type positions in the (Ca/Sr)O layers. Here, the F atoms would be tetrahedrally

coordinated to four Ca or Sr atoms and the T' structure would be formed initially, rather than the T-structure.

In summary, the work presented here shows that fluorination of $\text{Ca}_{2-x}\text{Sr}_x\text{CuO}_3$ with PVDF/PTFE gives $\text{Ca}_{2-x}\text{Sr}_x\text{CuO}_2\text{F}_2$ with the T'-structure across the complete range. This is the first time that a sample of $\text{Sr}_2\text{CuO}_2\text{F}_2$ with the T' (Nd_2CuO_4) structure has been made with no post-synthesis reduction required. The work suggests that it is the presence of interstitial F that stabilises the T-structure rather than the alkaline earth size as previously thought. Thus, since the fluorination of $\text{Ca}_{2-x}\text{Sr}_x\text{CuO}_3$ is non-oxidative, it results in $\text{Ca}_{2-x}\text{Sr}_x\text{CuO}_2\text{F}_2$ samples without interstitial F and therefore the T'-structure is observed.

Acknowledgements

We would like to thank EPSRC for funding (studentship to RH), and ISIS, Rutherford Appleton Lab, UK for the provision of neutron diffraction time. In addition we would like to thank Ron Smith for help with the collection of neutron diffraction data.

References

1. M. Al-Mamouri, P. P. Edwards, C. Greaves and M. Slaski, *Nature (London)* 1994, **369**, 382.
2. M. Al-Mamouri, P. Edwards, C. Greaves, P. R. Slater and M. Slaski, *J. Mater. Chem.*, 1995, **5**, 913.

3. P.R. Slater, P.P. Edwards, C. Greaves, I. Gameson, M. G. Francesconi, J. P. Hodges, M. Al-Mamouri, M. Slaski, *Physica C*, 1995, **241**, 151.
4. P.R. Slater, J.P. Hodges, M.G. Francesconi P.P. Edwards, C. Greaves, I. Gameson, M. Slaski, *Physica C*, 1995, **253**, 16.
5. B. Morosin, E.L. Venturini, J.E. Schirber, R.G. Dun, P.P. Newcomer, *Physica C*, 1995, **241**, 181.
6. J.E. Schirber, B. Morosin, E.L. Venturini, W.R. Bayless, *Physica C*, 1995, **245**, 270.
7. E.I. Ardashnikova, S.V. Lubarsky, D.I. Deisenko, R.V. Shpanchenko, E.V. Antipov, and G. Van Teendeloo, *Physica C*, 1995, **253**, 259.
8. B.N. Wani, S.J. Patwe, U.R.K. Rao, R.M. Kadam, M.D. Sastry, *Appl. Supercond.*, 1995, **3**, 321.
9. D.L. Novikov, A.J. Freeman, J.D. Jorgensen, *Phys. Rev. B*, 1995, **51**, 6675.
10. M.S. Islam, S. D'Arco, *Chem. Commun.*, 1996, 2291.
11. E. Z. Kurmaev, L. V. Elokhina, V. V. Fedorenko, S. Bartowski, M. Neumann, C. Greaves, P. P. Edwards, P. R. Slater and M. G. Francesconi, *J. Phys-Condens. Mat.*, 1996, **8**, 4847.
12. J. P. Hill, N.L. Allan, W.C. Mackrodt, *Chem. Commun.*, 1996, 2703.
13. M. Isobe, J.Q. Li, Y. Matsui, F. Izumi, Y. Kanke, E. Takayama-Muromachi, *Physica C*, 1996, **269**, 5.
14. Y. Jinling, L. Jingkui, R. Guanghui, Q. Yueling, S. Ying, T. Weihua, *Physica C*, 1996, **270**, 35.
15. B.N. Wani, L.L. Miller, B. J. Suh, F. Borsa, *Physica C*, 1996, **272**, 187.
16. S.C. Bhagava, B.N. Wani, *Solid State Commun.*, 1996, **99**, 825.

17. P.R. Slater, J.P. Hodges, M.G. Francesconi, C. Greaves, and M. Slaski, *J Mater. Chem.*, 1997, **7**, 2077.
18. S. D'Arco, M. S. Islam, *Phys. Rev. B*, 1997, **55**, 3141.
19. M. S. Islam, M. S. D. Read, S. D'Arco, *Faraday Discuss.*, 1997, **106**, 367.
20. J. L. Kissick, C. Greaves, P. P. Edwards, V. M. Cherkashenko, E. Z. Kurmaev, S. Bartkowski, M. Newman, *Phys. Rev. B*, 1997, **56** (5), 2831.
21. W.C. Mackrodt, H.J. Gotsis, N.L. Allan, *Ber. Bunsen-Ges. Phys. Chem.*, 1997, **101**, 1242.
22. M.G. Francesconi, P.R. Slater, J.P. Hodges, C. Greaves, P.P. Edwards, M. Al-Mamouri and M. Slaski, *J. Solid State Chem.*, 1998, **135**, 17.
23. S. Fujihara, Y. Masuda, J.S. Jin, T. Kimura, T. Tanabe, *Physica C*, 1997, **290**, 63.
24. C. Greaves, M.G. Francesconi, *Curr. Opin. Solid State Mater. Sci.*, 1998, **3**, 132.
25. C. Greaves, J.L. Kissick, M.G. Francesconi, L.D. Aikens, L.G. Gillie, *J. Mater. Chem*, 1999, **9**, 111.
26. J.H. Choi, W. Lee, S.J. Hwang, *Physica C*, 1999, **332**, 93.
27. C. Bersier, E.P. Stoll, P.F. Meier, T.A. Claxton, *J. Supercond.*, 2002, **15**, 399.
27. I.D.R. Moreira, R. Dovesi, *Phys. Rev. B*, 2003, **67**, 134513.
28. H. Oesterreicher, *Soidl State Commun.*, 2003, **127**, 563.
29. J. Sheng, K.B. Tang, Z.H. Liang, Y.K. Wang, D. Wang, W.Q. Zhang; *Mater. Chem. Phys.* 2009, 115, 483.
30. P.R. Slater, *J. Fluorine Chem.* 2002, **117**, 43.
31. F.J. Berry, X.Ren, R. Heap, P.R. Slater, M.F. Thomas; *Solid State Commun.* 2005, **134**, 621.

32. R. Heap, P.R. Slater, F.J. Berry, O. Helgason, A.J. Wright; *Solid State Commun.* 2007, **141**, 467.
33. Y. Kobayashi, M. Tian, M. Eguchi, T.E. Mallouk; *J. Amer. Chem. Soc.* 2009, **131**, 9849.
34. T. Sivakumar, J.B. Wiley; *Mater. Res. Bull.* 2009, **44**, 74.
35. T. Baikie, N.A. Young, M.G. Francesconi; *Prog. Solid State Chem.* 2007, **35**, 265.
36. A.C. Larson and R.B. Von Dreele, "General Structure Analysis System (GSAS)", Los Alamos National Laboratory Report LAUR 86-748 (2000).
37. D. R. Lines, M. T. Weller, D. B. Currie, D. M. Ogborne, *Mater. Res. Bull.*, 1991, **26**, 323.

Table 1: Atom positions and thermal parameters from Rietveld refinement of neutron diffraction data for $\text{Ca}_{2-x}\text{Sr}_x\text{CuO}_2\text{F}_2$ ($0 \leq x \leq 1.25$).

	x = 0.0	x = 0.25	x = 0.5	x = 0.75	x = 1.0	x = 1.25
Ca/Sr (0, 0, z) (4e)						
z	0.36508(7)	0.3645(1)	0.36504(5)	0.36534(7)	0.36531(9)	0.36602(9)
$U_1 (\times 100)/\text{\AA}^2$	0.65(1)	0.57(2)	0.692(9)	0.73(1)	0.67(1)	0.71(2)
Cu (0, 0, 0) (4a)						
$U_1 (\times 100)/\text{\AA}^2$	0.39(9)	0.36(2)	0.482(8)	0.49(1)	0.44(1)	0.47(1)
O (0, 0.5, 0) (4c)						
$U_1 (\times 100)/\text{\AA}^2$	*	*	*	*	*	*
$U_{11}(\times 100)/\text{\AA}^2$	0.84(2)	0.57(4)	0.89(2)	0.90(2)	0.89(3)	0.75(3)
$U_{22}(\times 100)/\text{\AA}^2$	0.25(2)	0.39(4)	0.34(2)	0.24(2)	0.16(3)	0.08(3)
$U_{33}(\times 100)/\text{\AA}^2$	1.15(3)	1.11(5)	1.27(2)	1.37(3)	1.51(4)	1.65(5)
F (0, 0.5, 0.25) (4d)						
$U_1 (\times 100)/\text{\AA}^2$	*	*	*	*	*	*
$U_{11}(\times 100)/\text{\AA}^2$	0.89(2)	0.99(3)	1.31(2)	1.44(2)	1.52(3)	1.73(4)
$U_{22}(\times 100)/\text{\AA}^2$	0.89(2)	0.99(3)	1.31(2)	1.44(2)	1.52(3)	1.73(4)
$U_{33}(\times 100)/\text{\AA}^2$	1.06(3)	1.31(6)	1.52(3)	1.59(4)	1.32(5)	1.34(5)
a (Å)	3.85697(4)	3.87126(7)	3.88705(3)	3.90212(4)	3.91680(5)	3.93071(6)
c (Å)	11.8274(2)	11.9496(4)	12.0702(2)	12.1949(2)	12.3144(3)	12.4282(3)

R_{wp}	0.0170	0.0356	0.0177	0.0185	0.0225	0.0181
R_p	0.0327	0.0469	0.0320	0.0320	0.0364	0.0275
χ^2	4.219	12.67	3.224	4.03	6.647	9.099

* Anisotropic thermal parameters

Table 2: Atom positions and thermal parameters from Rietveld refinement of X-ray diffraction data for $\text{Ca}_{2-x}\text{Sr}_x\text{CuO}_2\text{F}_2$ ($1.5 \leq x \leq 2.0$).

	x = 1.5	x = 1.75	x = 2.0
Ca/Sr (0, 0, z) (4e)			
z	0.3670(2)	0.3666(2)	0.3662(3)
$U_1 (\times 100)/\text{\AA}^2$	0.54(9)	0.58(8)	0.4(1)
Cu (0, 0, 0) (4a)			
$U_1 (\times 100)/\text{\AA}^2$	0.9(2)	1.0(2)	0.9(3)
O (0, 0.5, 0) (4c)			
$U_1 (\times 100)/\text{\AA}^2$	0.2(5)	0.8(5)	4(1)
F (0, 0.5, 0.25) (4d)			
$U_1 (\times 100)/\text{\AA}^2$	0.7(4)	0.4(4)	-0.5(7)
a (Å)	3.9452(2)	3.9593(2)	3.9739(3)
c (Å)	12.549(1)	12.6733(9)	12.782(1)
R_{wp}	0.0770	0.0749	0.0749
R_{p}	0.0611	0.0588	0.0592
χ^2	1.303	1.21	1.232

Figure 1: T'-structure (Nd_2CuO_4 structure)

Figure 2: T-structure (La_2CuO_4 structure)

Figure 3: XRD patterns for the series $\text{Ca}_{2-x}\text{Sr}_x\text{CuO}_3$

Figure 4: XRD patterns for the series $\text{Ca}_{2-x}\text{Sr}_x\text{CuO}_2\text{F}_2$ ((Ca/Sr) F_2 impurities marked with *)

Figure 5: Observed, calculated and difference neutron diffraction profiles for $\text{Ca}_2\text{CuO}_2\text{F}_2$
(Lower tick marks): middle tick-marks: CaO, upper tick-marks: CaF_2

Figure 6. Variation in cell parameters (a, c) across the series $\text{Ca}_{2-x}\text{Sr}_x\text{CuO}_2\text{F}_2$

Figure 7. Variation in (a) Cu-O bond lengths, (b) Ca/Sr-O bond lengths, and (c) Ca/Sr-F bond lengths across the series $\text{Ca}_{2-x}\text{Sr}_x\text{CuO}_2\text{F}_2$

Figure 8. The Structure of $\text{Ca}_{2-x}\text{Sr}_x\text{CuO}_3$

Figure 9. The change in the c parameter upon fluorination of the $\text{Ca}_{2-x}\text{Sr}_x\text{CuO}_3$ series (cell parameters for $\text{Ca}_{2-x}\text{Sr}_x\text{CuO}_3$ adapted from those of Lines *et al.* [37])

Figure 1

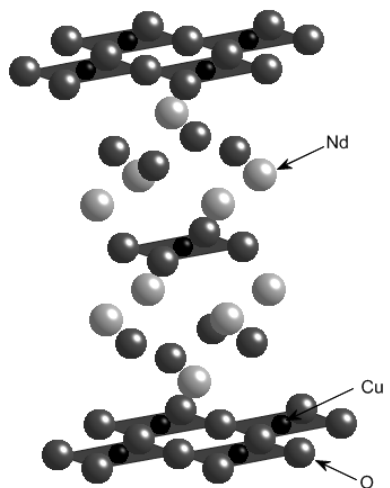


Figure 2

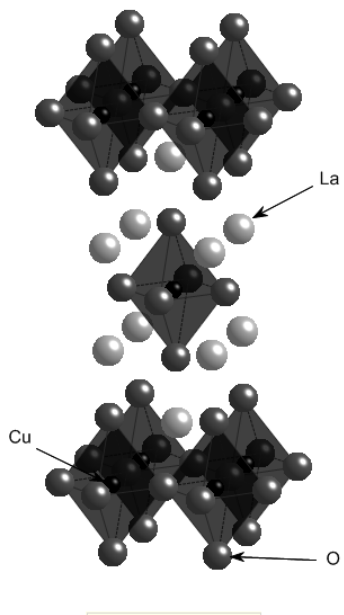


Figure 3.

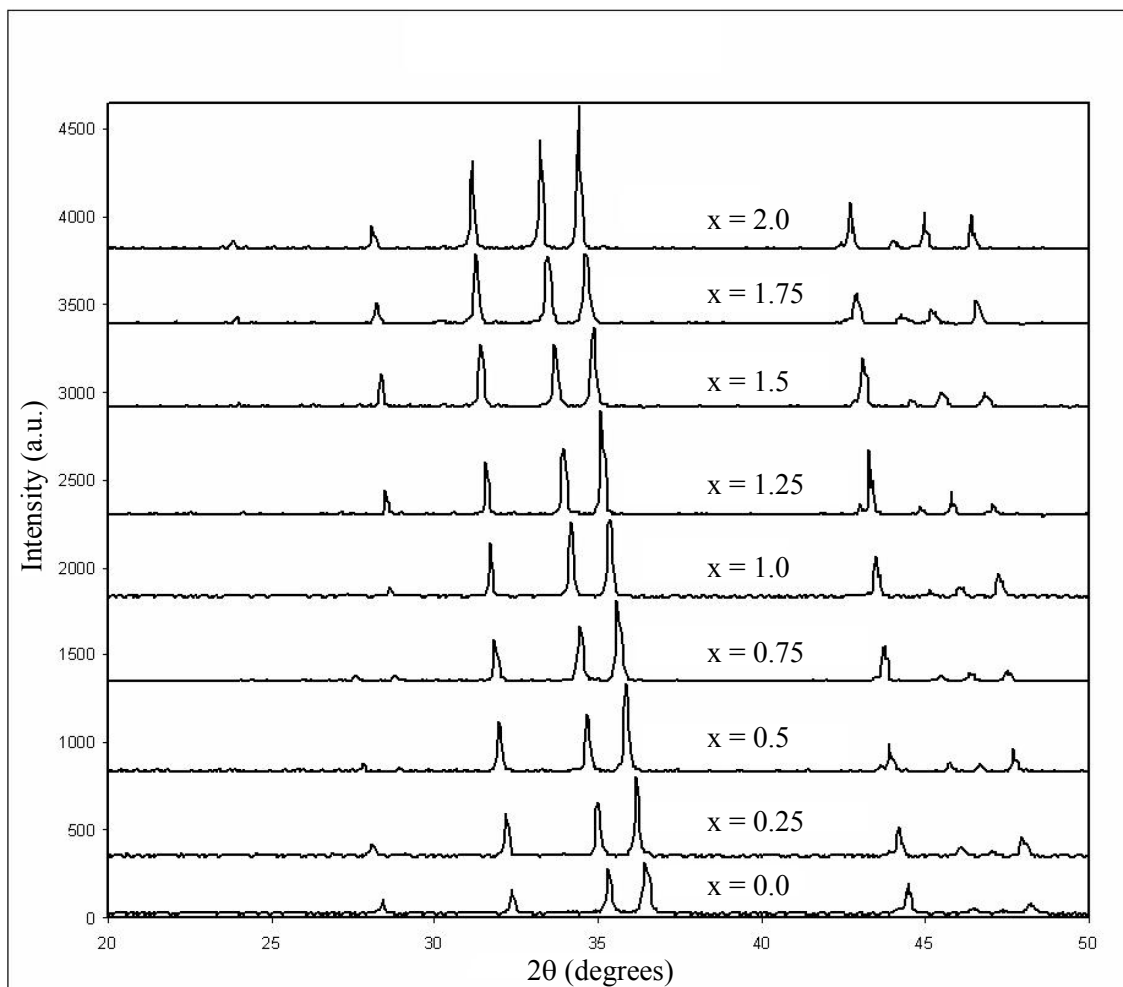


Figure 4

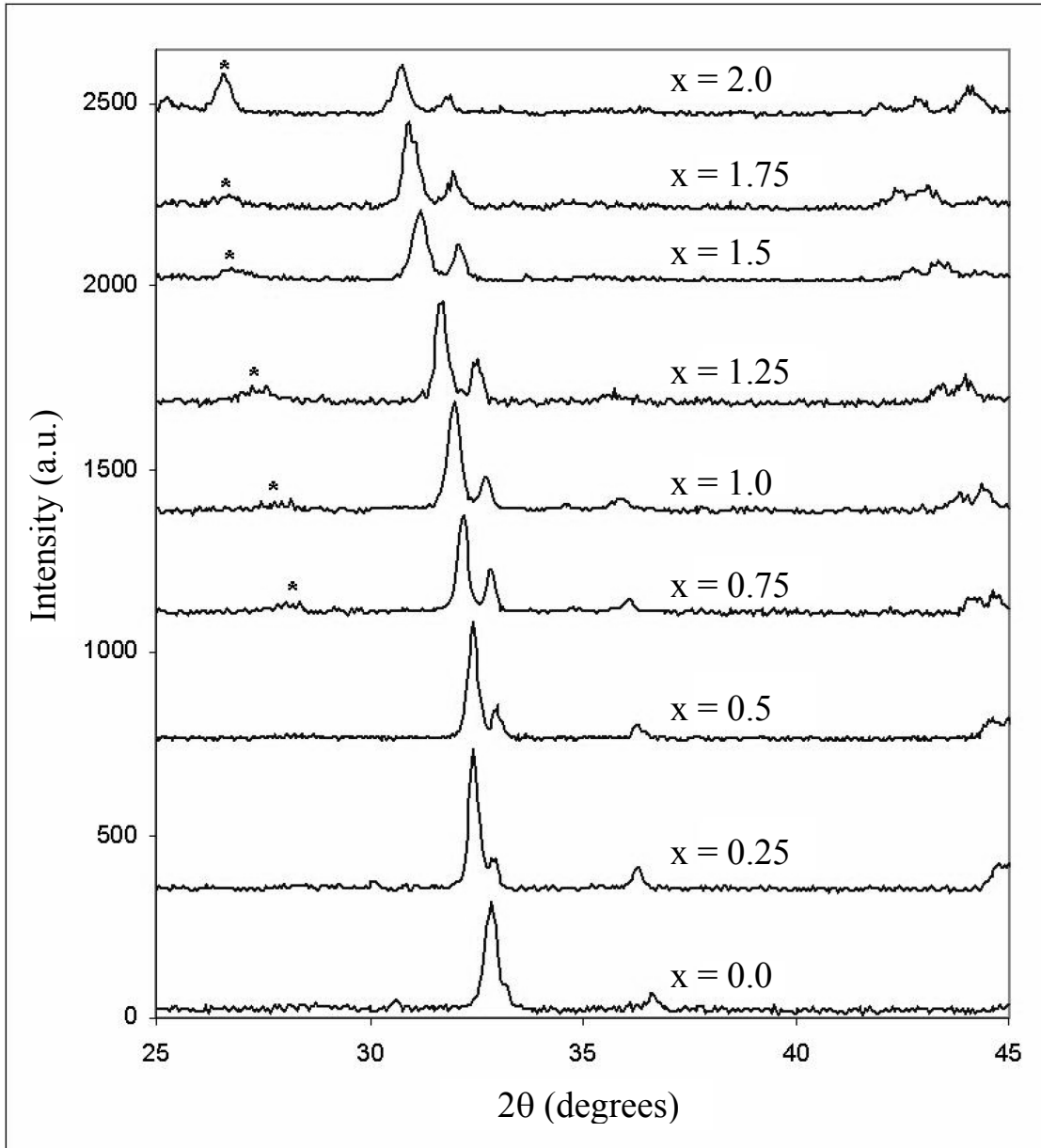


Figure 5.

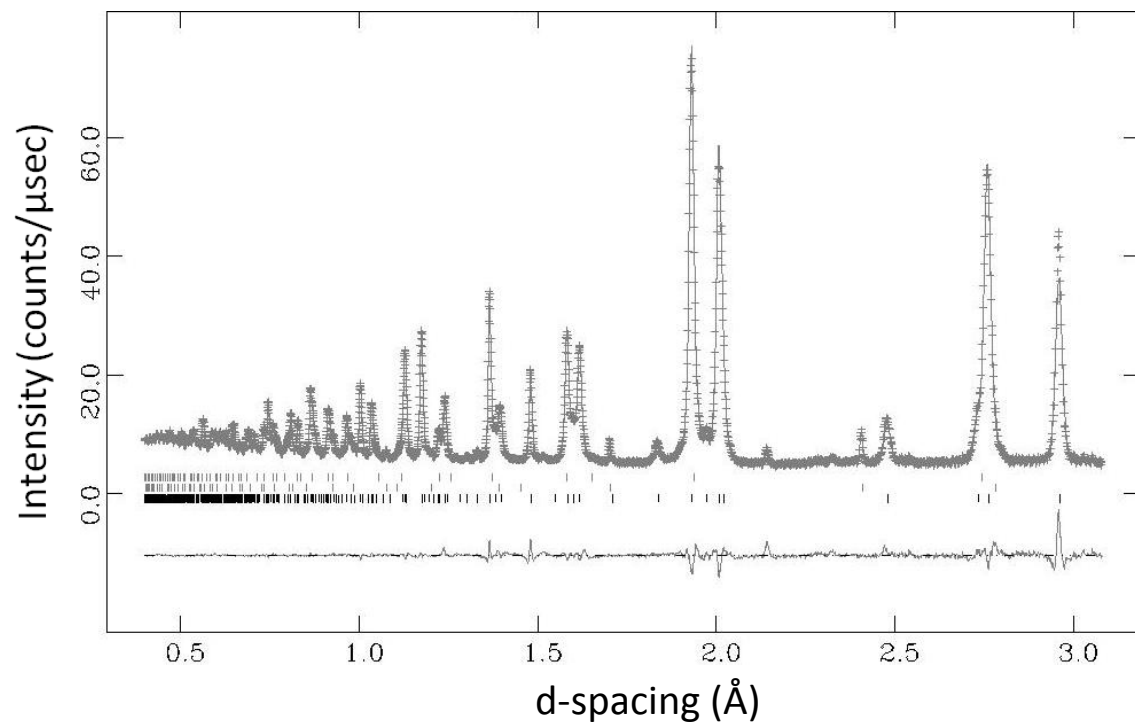
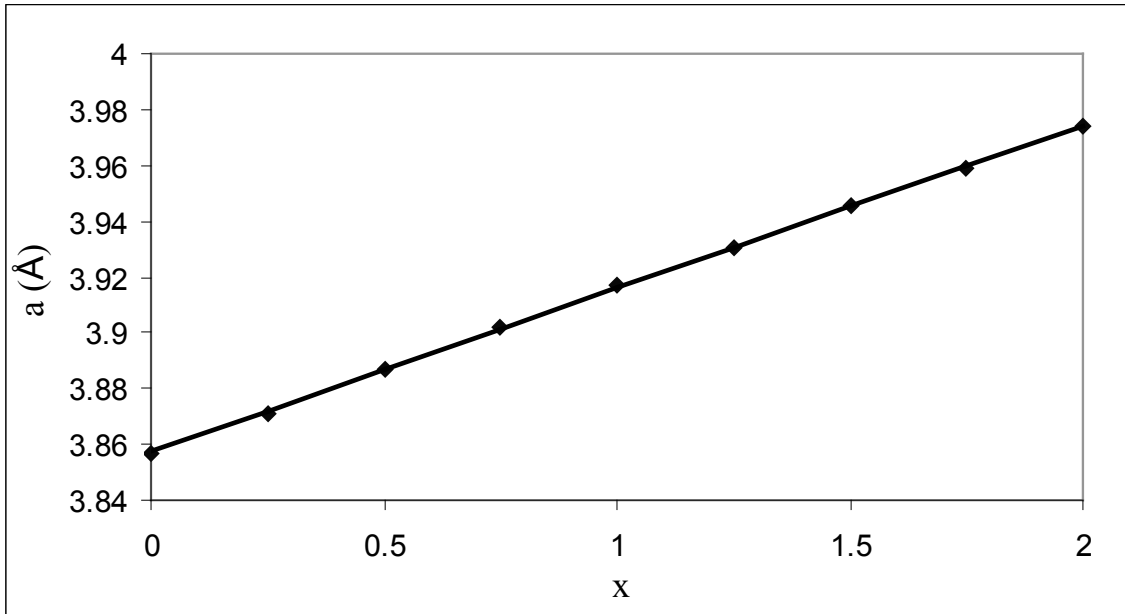


Figure 6. (a)



(b)

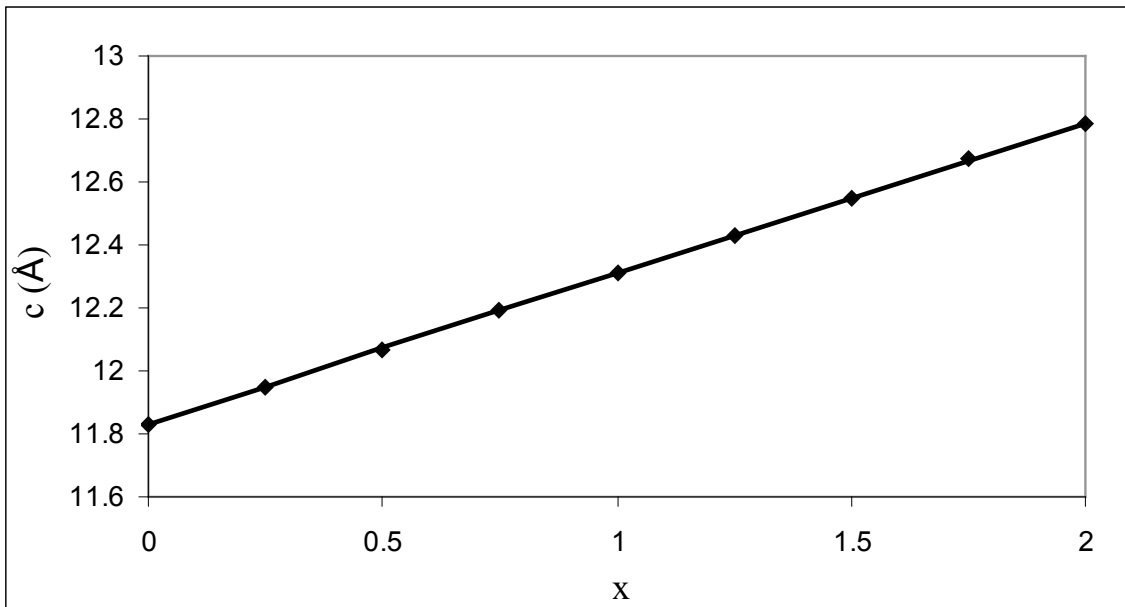
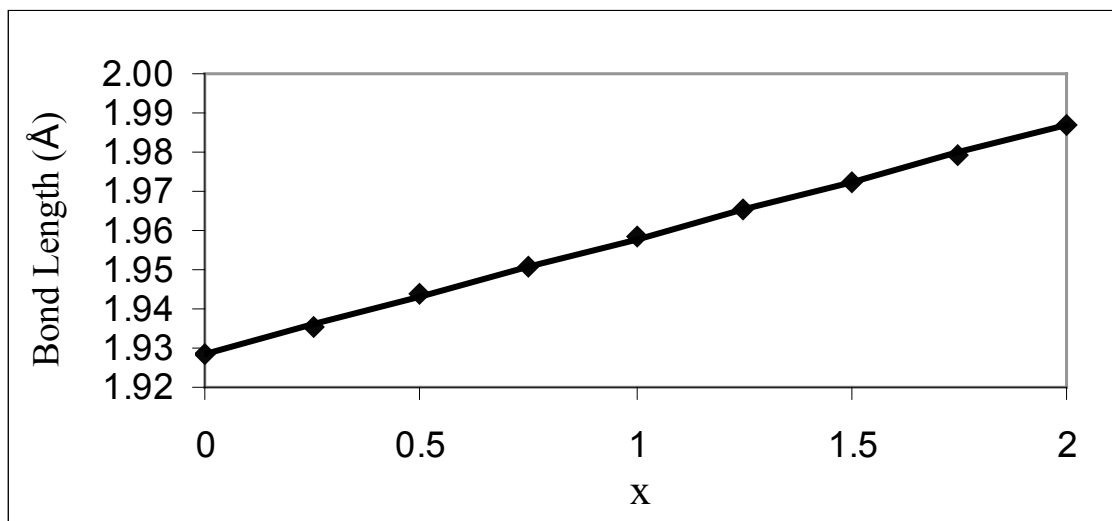
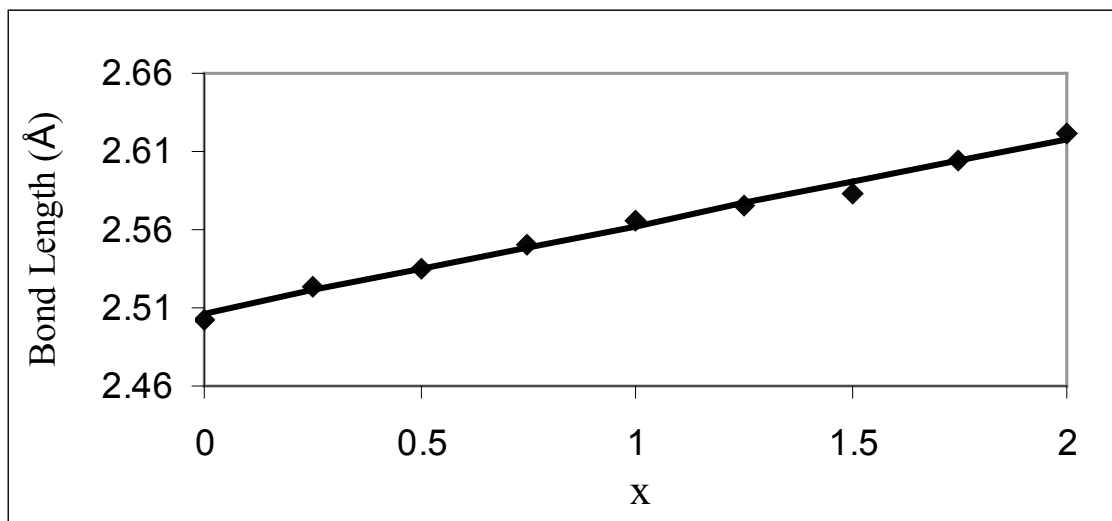


Figure 7(a).



(b)



(c)

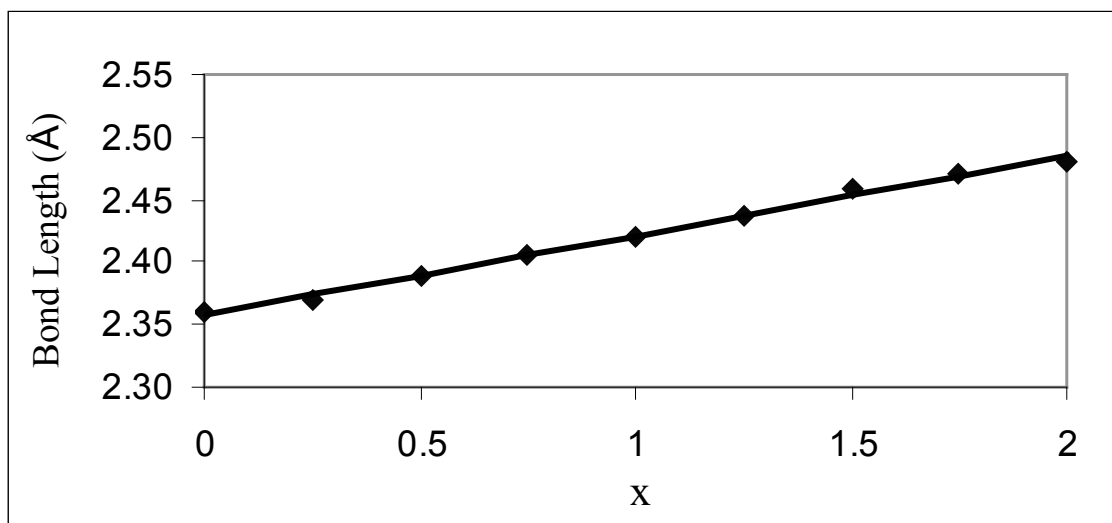


Figure 8.

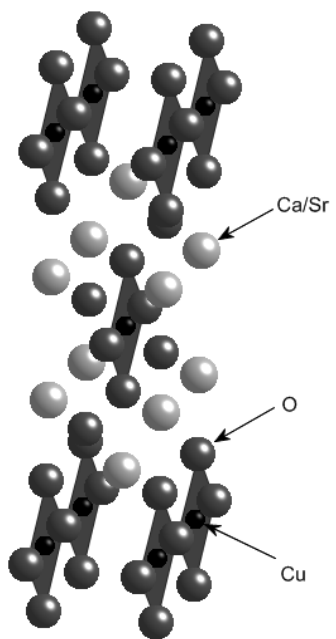


Figure 9.

